Monthly Notices of the ROYAL ASTRONOMICAL SOCIETY

MNRAS **539,** 2242–2247 (2025) https://doi.org/10.1093/mnras/staf636
Advance Access publication 2025 April 17

Search for dark matter annihilation to γ-rays from nearby galaxy clusters with *Fermi*-LAT data

Shang Li* and Feng Han
School of Physics and Optoelectronic Engineering, Anhui University, Hefei 230601 , China

Accepted 2025 April 9. Received 2025 April 9; in original form 2025 January 12

ABSTRACT

In this work, we adopt 16 yr of *Fermi*-LAT data to search for γ-ray signal from dark matter annihilation in 16 nearby galaxy clusters. The NFW profile is applied to model the dark matter distribution. No significant ($> 5\sigma$) γ-ray signal is found in the scenarios of dark matter annihilations. However, the peak test statistic (TS) values are larger than 16.0 for Coma and Perseus clusters. Further analyses strongly indicate that the γ-ray emission of the Coma region is irrelevant to the dark matter annihilations. For Perseus cluster, the best-fitting TS value is ~ 20.0 for $\chi\chi \rightarrow \tau^+\tau^-$ at $m_\chi \sim 38$ GeV, but the corresponding $\langle\sigma v\rangle$ is in conflict with the constraint from dwarf spheroidal galaxies. Meanwhile, the peak TS value of the possible excess from Perseus is not increasing with time continually. The true origin of the potential signal is still unclear.

Key words: galaxies: clusters: general – gamma-rays: galaxies: clusters – dark matter – galaxies: clusters: individual: Coma – galaxies: clusters: individual: Perseus.

1 INTRODUCTION

Astrophysical and cosmological evidences show that non-baryonic cold dark matter (DM) accounts for 84 per cent of the matter density of the Universe (Planck Collaboration XIII 2016). At the moment, the nature of dark matter is still unclear. Among the many candidates of DM particle, one of the possible candidates is a weakly interacting massive particles (WIMPs) (Bertone, Hooper & Silk 2005; Hooper & Profumo 2007; Feng 2010), since there is no observational evidence that dark matter is a WIMP. WIMPs may annihilate or decay into Standard Model particles and eventually produce γ-rays, cosmic rays, and so on. These γ-ray signals may be detected by some telescopes, such as *Fermi*-LAT (Atwood et al. 2009) and *DAMPE* (Chang et al. 2017).

Galaxy clusters (GCls) are the largest and most massive gravitationally bound systems in the Universe, which contains a large amount of DM. In addition, the N-body numeric simulations in the ΛCDM cosmology showed that there will be a large number of subhaloes in the DM halo of a cluster size (Diemand et al. 2008; Springel et al. 2008). Due to the flux of DM annihilation is proportional to $\rho^2(r)$, where $\rho(r)$ is the DM density, these subhaloes can enhance the DM signal significantly compared to the smooth DM distribution. Therefore, GCls may be one of the excellent targets in searching for signatures of DM annihilation (Jeltema, Kehayias & Profumo 2009; Pinzke, Pfrommer & Bergström 2009).

Since the launch of the *Fermi*-LAT satellite, great efforts have been paid to look for DM annihilation to γ-ray signals from GCls, no identified signal has been found so far and gave some constraints on the parameters of DM (Ackermann et al. 2010, 2015b; Dugger, Jeltema & Profumo 2010; Han et al. 2012; Huang, Vertongen & Weniger 2012; Thorpe-Morgan et al. 2021; Manna & Desai 2024). Moreover, some interesting signals have been found in the literatures. A very significant spatially extended γ-ray emission in Coma region was reported by Xi et al. (2018) and confirmed in some literatures (Liang et al. 2018; Thorpe-Morgan et al. 2021; Baghmanyan et al. 2022; Chen et al. 2024,). However, the origin of this emission is still under debate. Searching for dark matter signals from 49 clusters was performed and reported signals at 2.5σ–3.0σ (Di Mauro et al. 2023). However, the best-fitting values of the cross-sections are excluded by the constraints from dwarf spheroidal galaxies (Ackermann et al. 2015a). In addition, a tentative monochromatic signal at the energy of ~ 43 GeV is found from 16 nearby GCls (Liang et al. 2016; Shen, Xia & Fan 2021). Recently, this γ-ray line signal at ~ 43 GeV is confirmed by 15.5 yr of *Fermi*-LAT data with a global significance of $\sim 4.3\sigma$ (Fan et al. 2024). The true origin of this signal is uncertain. In this paper, we analyse 16 yr of *Fermi*-LAT data to search for continual γ-ray emission of DM annihilation in these galaxy clusters. The samples are listed in Table 1.

2 DATA ANALYSIS

In this paper, we use the *Fermi*-LAT Pass 8 data (P8R3_CLEAN_V3, FRONT+BACK) in the energy range between 500 MeV and 500 GeV. The software *Fermitools* is applied to carry out the data analysis. We consider 16 yr data from 2008 August 4 to 2024 August 4 [i.e. Mission Elapsed Time (MET) range 239557417–744479021]. To reduce the contamination from the Earth's limb, only the photons with zenith angles less than 100° are considered. The recommended quality-filter cuts (DATA_QUAL==1 && LAT_CONFIG== = 1) are adopted to ensure the data quality.

* E-mail: lishang@ahu.edu.cn

Table 1. Parameters of the GCls. The redshift z, right ascension α, and declination δ in J2000 epoch of each GCl are taken from Chen et al. (2007). The virial masses M_{200} are taken from the reference (Fan et al. 2024). θ_{200} is the angular size of virial radii R_{200}. J ($J_{\rm sub}$) is the J-factor given the NFW profile of the clusters without (with) the substructures. TS (TS$_{\rm sub}$) is the peak TS value of each cluster without (with) the substructures.

GCl	α (deg)	δ (deg)	z	M_{200} ($10^{14}M_\odot$)	R_{200} (Mpc)	θ_{200} (deg)	$\log_{10}(J)$ (GeV^2 cm^{-5})	TS	$\log_{10}(J_{\rm sub})$ (GeV^2 cm^{-5})	TS$_{\rm sub}$
Virgo	187.704	12.391	0.0038	1.050	0.972	3.41	17.93	0.3	19.05	0.3
Fornax	54.669	−35.310	0.0046	1.196	1.015	2.94	17.82	3.3	18.94	2.1
Ophiuchus	258.111	−23.363	0.0280	34.691	3.096	1.45	17.69	3.6	18.71	3.3
M49	187.444	7.997	0.0038	0.460	0.738	2.59	17.61	0.8	18.73	0.0
A3526	192.200	−41.309	0.0103	3.156	1.400	1.80	17.51	4.2	18.62	1.6
A1060	159.178	−27.521	0.0114	2.309	1.261	1.47	17.30	6.2	18.41	8.2
Coma	194.947	27.939	0.0232	9.004	1.977	1.12	17.27	17.9	18.33	20.6
NGC4636	190.708	2.688	0.0037	0.155	0.514	1.85	17.22	2.3	18.32	3.5
AWM7	43.623	41.578	0.0172	4.491	1.571	1.21	17.23	0.8	18.32	1.7
A1367	176.190	19.703	0.0216	6.733	1.796	1.09	17.20	1.9	18.28	2.7
NGC5813	225.299	1.698	0.0064	0.385	0.695	1.44	17.10	0.5	18.20	2.0
A2877	17.480	−45.922	0.0241	6.166	1.743	0.95	17.08	0.0	18.15	1.8
S636	157.421	−35.326	0.0093	0.763	0.872	1.24	17.04	5.2	18.15	10.6
A3627	243.555	−60.843	0.0163	4.487	1.571	1.27	17.27	4.3	18.36	2.8
Perseus	49.946	41.515	0.0183	5.476	1.678	1.21	17.26	20.0	18.34	8.5
3C129	72.560	45.026	0.0223	4.796	1.604	0.95	17.03	0.0	18.12	0.0

The background model is generated by `make4FGLxml.py`.[1] All 4FGL-DR4 (Abdollahi et al. 2022) sources within 15° around the centre of each target and the recommended diffuse components (gll_iem_v07.fits and iso_P8R3_CLEAN_V3_v1.txt) are included. We perform a binned likelihood analysis.[2] In this process, the spectral parameters of the 4FGL-DR4 sources around 5° radius of the centre and the normalizations of the two diffuse backgrounds are set free. The *gtlike* tool and the *MINUIT* algorithm are used to get the best-fitting values. The significance of the target can be quantified by the test statistic (TS), whose expression is $TS = -2\ln(L_0/L)$ (Mattox et al. 1996), where L and L_0 are the best-fitting likelihood values for the model with and without the target, respectively. The residual TS map of each target is generated by the *gttsmap* tool. Any excess outside the virial radius of each target with a TS value larger than 16.0 is regarded as a point source. We add these point sources into the model with a power law (PL, $\mathrm{d}N/\mathrm{d}E \propto E^{-\Gamma}$, Γ is the spectral photon index) spectral model and their locations are derived by the *gtfindsrc* tool. In the following analyses, these new point sources are included in the models.

3 SEARCH FOR DARK MATTER EMISSION

Galaxy cluster is an ideal target for indirect detection of DM. The expected γ-ray flux from DM annihilation is (Jungman, Kamionkowski & Griest 1996; Bertone et al. 2005; Hooper & Profumo 2007; Feng 2010)

$$\Phi(E_\gamma) = \frac{\langle\sigma v\rangle}{8\pi m_\chi^2}\frac{\mathrm{d}N_\gamma}{\mathrm{d}E_\gamma} \times J, \tag{1}$$

where m_χ, $\langle\sigma v\rangle$, $\mathrm{d}N_\gamma/\mathrm{d}E_\gamma$ are the rest mass, thermal averaged annihilation cross-section, and the differential γ-ray production by each annihilation of the DM particle. The term $J = \int\rho^2(r)\mathrm{d}l\mathrm{d}\Omega$ is the integral of the square of DM density in the line-of-sight (i.e. J-factor).

The main DM halo of each cluster can be described with a Navarro-Frenk-White (NFW) profile (Navarro, Frenk & White 1996, 1997):

$$\rho_{\rm NFW}(r) = \frac{\rho_0}{(\frac{r}{r_s})(1+\frac{r}{r_s})^2}, \tag{2}$$

where ρ_0 is the central density and r_s is the scale radius. According to the concentration–mass (c–M) relation (Sánchez-Conde & Prada 2014)[3], we can derive the concentration parameter c_{200} with the M_{200}.

Similar to Di Mauro et al. (2023), the virial radius R_{200} can be obtained from M_{200} as follows:

$$R_{200} = \left(\frac{3M_{200}}{4\pi\Delta_{200}\rho_{\rm crit}}\right)^{1/3}, \tag{3}$$

where Δ_{200} is the overdensity factor, which is 200 in this case. The critical density $\rho_{\rm crit}$ can be calculated by the Hubble parameter $H(z)$ according to the equation:

$$\rho_{\rm crit} = \frac{3H^2(z)}{8\pi G}, \tag{4}$$

where $H(z) \equiv H_0\sqrt{\Omega_M(1+z)^3+1-\Omega_M}$ for flat ΛCDM. We take $H_0 = 70\ \mathrm{km\,s^{-1}\,Mpc^{-1}}$ and $\Omega_{\rm M} = 0.3$. The scale radius in equation (2) is obtained by $r_s = R_{200}/c_{200}$. We can derive the scale density ρ_0 from c_{200} as follows:

$$\rho_0 = \frac{2\Delta_{200}\rho_{\rm crit}c_{200}}{3f(c_{200})}, \tag{5}$$

where $f(c_{200}) = \frac{2}{(c_{200}^2)}\left[\ln(1+c_{200}) - \frac{c_{200}}{1+c_{200}}\right]$.

Galaxy clusters are expected to host a large number of subhaloes. We will use the `CLUMPY v3`[4] software (Charbonnier, Combet & Maurin 2012; Bonnivard et al. 2015; Hütten, Combet & Maurin 2019) to consider the impact of the substructures in the cluster's DM density distributions (Diemand, Kuhlen & Madau 2007; Springel et al. 2008). In order to sufficiently model the subhaloes, we assume a

[1] https://fermi.gsfc.nasa.gov/ssc/data/analysis/user/make4FGLxml.py
[2] https://fermi.gsfc.nasa.gov/ssc/data/analysis/scitools/likelihood_tutorial.html
[3] If the concentration–mass (c–M) relation in Moliné et al. (2017) is used, the results are very similar and not presented in this paper.
[4] https://clumpy.gitlab.io/CLUMPY/v3.1.1/_downloads/975332ce6631f0956830ed27431f3b25/CLUMPY_v2018.06.CPC.tar.gz

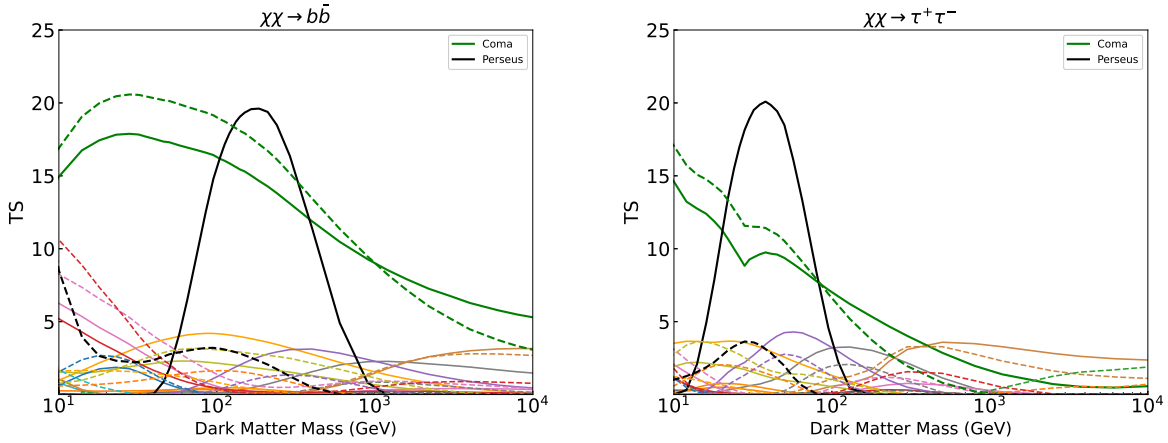

Figure 1. TS as a function of the DM particle mass for the 16 GCls listed in Table 1 assuming DM annihilating through the $b\bar{b}$ (left) or $\tau^+\tau^-$ (right) channels. The dotted and solid lines are denoted the results with and without the substructures, respectively.

mass distribution function of $\mathrm{d}N_{\rm sub}/\mathrm{d}M \propto M^{-1.9}$. The minimal mass of subhalo is assumed to be $10^{-6}M_{\odot}$ and the maximum subhalo mass is 0.01 per cent of the halo mass. These parameters are similar to the MED model in Di Mauro et al. (2023). We take the (c–M) relation defined in Moliné et al. (2017) to describe subhalo DM profiles. We use the Einasto profile to model the spatial distribution ($\mathrm{d}N_{\rm sub}/\mathrm{d}V$) of the substructures.

4 RESULTS

The *DMFitFunction* contained in *Fermitools* is applied to fit for putative DM components (Jeltema & Profumo 2008). We consider two typical DM annihilation channels ($b\bar{b}$ and $\tau^+\tau^-$) and fit the data for a series of DM masses from 10 GeV to 10 TeV. The TS value as a function of DM mass for clusters are shown in Fig. 1. We summarized the peak TS values in Table 1. No significant (i.e. TS > 25) signal is found in our analyses. However, the local significance of the γ-ray emission in the directions of two galaxy clusters (Coma and Perseus) are larger than 4σ. In the following, we will further investigate the two clusters (Coma and Perseus).

4.1 Coma

The best-fitting TS value of Coma is $\sim$ 17.9 (20.6) corresponding to a DM mass of $m_\chi \sim 30$ GeV for $\chi\chi \to b\bar{b}$. In case of $\chi\chi \to \tau^+\tau^-$, the peak TS value is $\sim$ 14.6 (17.0) at $m_\chi \sim 10$ GeV. The TS values in the brackets are obtained by the NFW model with substructures. The peak TS values are similar for the two situations. If the signal is due to DM annihilation, the signal is expected to be steady and the expected TS will increase with time. Hence, we repeat the data analysis for the 4, 8, and 12 yr of *Fermi*-LAT data without substructures and the DM mass is fixed at 30 (10) GeV for $\chi\chi \to b\bar{b}$ ($\tau^+\tau^-$), the TS values are shown in Fig. 2. As is shown, the TS value rapidly increased in the last few years. In addition, we perform a data analysis for the second 8 yr (from 2016 August 4 to 2024 August 4), the peak TS value is $\sim$ 22.0 (17.5) for $\chi\chi \to b\bar{b}$ ($\tau^+\tau^-$), which is 5 times larger than the TS value of the first 8 yr. These facts indicate that the signal is not a stable emission and not consistent with the expectation of DM annihilation.

In addition, we generate the residual TS map of the Coma region (see Fig. 3) according to the background model only. The white dashed circle shows the 1.12° virial radius of the Coma. According

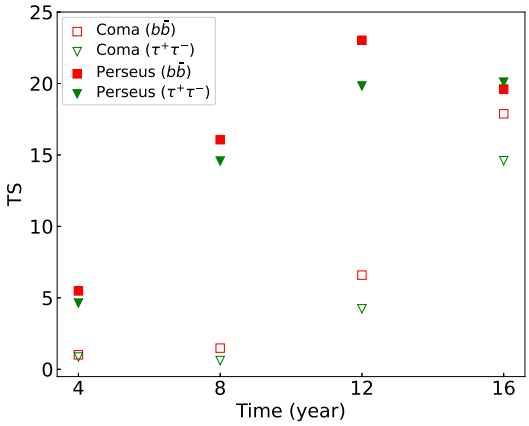

Figure 2. The TS values of the potential signals in the direction of Coma and Perseus for $\chi\chi \to b\bar{b}$ and $\tau^+\tau^-$ in four different time intervals without the substructures.

to Fig. 3, a residual structure appears within the Coma region, and the position of the peak TS value is near the centre of Coma. We model the residual emission as a point source (PS) with a PL spectra. The TS value is $\sim$ 23.3 with $\Gamma = 2.48 \pm 0.26$ and the average photon flux is $\sim (2.15 \pm 0.70) \times 10^{-10}$ph cm^{-2}s^{-1}. In addition, a 1-yr bin γ-ray light curve is extracted for the PS model. When one bin with TS < 4, the 95 per cent confidence level (C.L.) upper limit is derived by the *pyLikelihood UpperLimits* tool. From Fig. 4, the TS values in most time bins are very small (< 4) and the γ-ray signals are mainly distributed in the second half of the entire period. To quantify the significance of the variability, the method in Nolan et al. (2012) is applied to calculate the variability index and then to obtain the significance of the variability. The variability significance of the one-year bin light curve is about 3.6σ for the entire 16 yr data, which is not consistent with the expectation of DM annihilation.

Furthermore, we remove the 4FGL J1256.9+2736 (4FGL J1256.9+2736 is a point source in the catalogue of 4FGL-DR4 and located within the virial radius of the Coma cluster) from the model and the residual TS maps of the two periods (from 2008 August 4 to 2016 August 4 and from 2016 August 4 to 2024 August 4) are shown in Fig. 5. For the first period, the TS value is very small in the centre of Coma and the residual γ-ray excesses are located at the south–west of the Coma region (see the left panel of Fig. 5), which

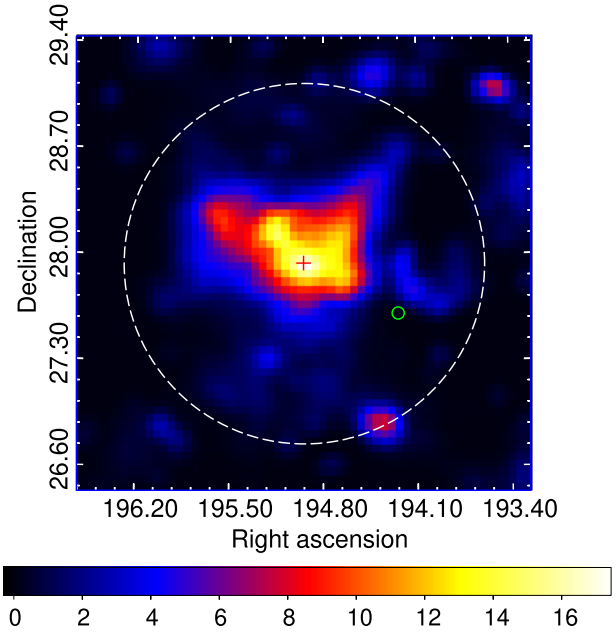

Figure 3. The residual TS map of 3° × 3° with 0.05° per pixel centred at the Coma. The white dashed circle is the region subtended by the virial radius ($\theta_{200} = 1.12°$). The green circle is the symbol of 4FGL J1256.9+2736 and the red cross represents the center position of Coma.

is similar to the previous results (Liang et al. 2018; Xi et al. 2018; Baghmanyan et al. 2022). However, the residual emission is located at the centre of Coma cluster and the peak TS value is ∼ 30 (see the right panel of Fig. 5), which is coinciding with above results. While the TS value is very small in the direction of 4FGL J1256.9+2736. The γ-ray emission in the region of Coma located at different areas for the two periods, which suggests that the γ-ray emissions are not originated from DM annihilation.

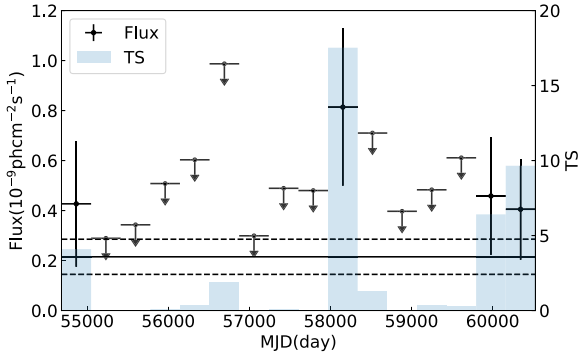

Figure 4. One-year bin γ-ray light curve of the target. The horizontal solid line represents the average flux of the entire 16 yr data and its 1σ flux error is marked by the dashed lines.

4.2 Perseus

The peak TS value is ∼ 19.5 (20.0) for the annihilation channel $\chi\chi \to b\bar{b}$ ($\tau^+\tau^-$) and the corresponding DM mass is ∼ 185 (38) GeV for Perseus (no substructures). If the γ-ray signal is originated from DM annihilations, the required cross-sections are $\langle\sigma v\rangle_{\chi\chi\to b\bar{b}} \sim 1.0 \times 10^{-22}\mathrm{cm}^3\mathrm{s}^{-1}$ for $\chi\chi \to b\bar{b}$ and $\langle\sigma v\rangle_{\chi\chi\to\tau^+\tau^-} \sim 2.2 \times 10^{-23}\mathrm{cm}^3\mathrm{s}^{-1}$ for $\chi\chi \to \tau^+\tau^-$ to interpret the signals with the J-factor in Table 1 (no substructures). However, such $\langle\sigma v\rangle$ is much larger than the current most stringent limits for DM by the stacked analysis of dwarf spheroidal galaxies (Ackermann et al. 2015a). At the same time, a known γ-ray source (4FGL J0319.8+4130) in 4FGL-DR4 catalogue is very close to the centre of Perseus, which is a very strong γ-ray source and the counterpart is a radio galaxy (NGC 1275) (Kataoka et al. 2010). Owing to the expected emission is much more concentrated on the centre of the NFW model, the γ-ray flux is very large and the flux may mainly come from NGC 1275, which leads to the very large cross-sections. If we consider the effect of substructures, the largest TS value is ∼ 8.5 (3.6) at $m_\chi \sim$ 10 (30) GeV for $\chi\chi \to b\bar{b}$ ($\tau^+\tau^-$), which is less than the TS value of no substructures.

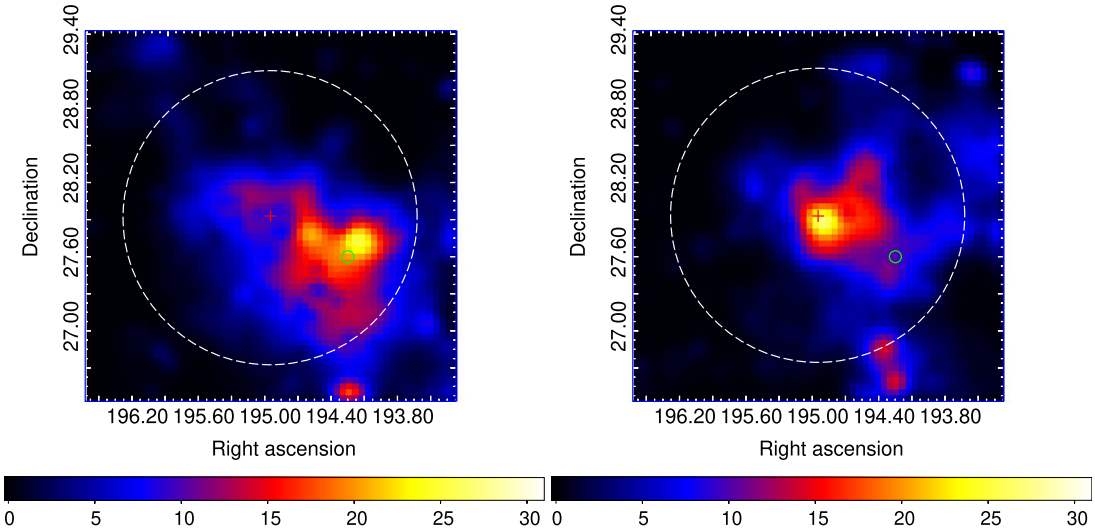

Figure 5. The residual TS maps of the Coma region for different epochs: (left) from 2008 August 4 to 2016 August 4, (right) from 2016 August 4 to 2024 August 4. The two panels represent 3° × 3° with 0.05° per pixel. The white dashed circle is the region of virial radius. The red cross is the centre position of the Coma cluster and the green circle is the position of 4FGL J1256.9+2736.

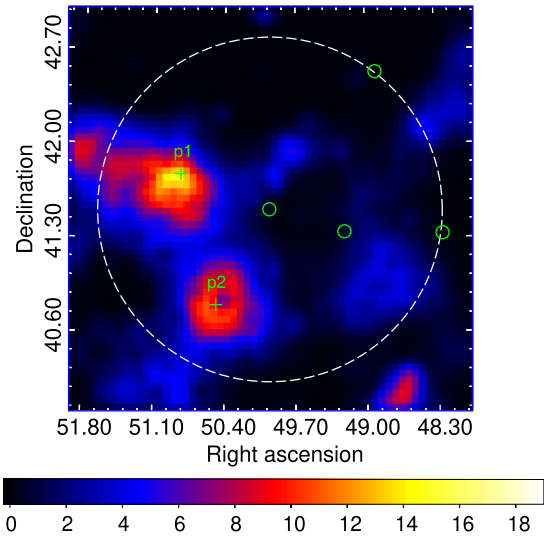

Figure 6. The residual TS map of the Perseus region. The map has a dimension of $3^\circ \times 3^\circ$ and a resolution of 0.05° per pixel. The virial radius ($\theta_{200} = 1.21^\circ$) is marked by the white dashed circle. The green circles represent the sources in the catalogue of 4FGL-DR4 and the two green crosses indicate the locations of p1 and p2.

Similarly, we also perform the data analysis for 4, 8, and 12 yr of *Fermi*-LAT data, the results are presented in Fig. 2. Clearly, the TS value of the signal is not increasing with the time in the last 4 yr, which is not consistent with the expectation of DM annihilation. At present, the signal is still weak and the possibility of the origin of statistical fluctuations cannot be ruled out.

We display the residual TS map of the Perseus region in Fig. 6. Four known γ-ray sources in 4FGL-DR4 catalogue are located in the $3^\circ \times 3^\circ$ region. The white dashed circle shows the virial radius. Obviously, there are some excesses within the virial region, which seem to be two point-like sources. Their positions are (R.A., Dec) $= (50.84^\circ, 41.77^\circ)$ and (R.A., Dec) $= (50.48^\circ, 40.80^\circ)$. The two point sources denoted as green crosses in Fig. 6, namely p1 and p2. After adding the two sources into the model, the largest TS value drops to ~ 15.0 (16.2) at $m_\chi \sim 200$ (40) GeV for $\chi\chi \to b\bar{b}$ ($\tau^+\tau^-$) without substructures.

4.3 Limit on $\langle \sigma v \rangle$

We derive the constraints on $\langle \sigma v \rangle$ of DM annihilating to $b\bar{b}$ and $\tau^+\tau^-$. To do this, a standard binned likelihood analysis is performed to determine the parameters of background sources and then the parameters are fixed at the best-fitting values. We take the similar method in Di Mauro et al. (2023) to obtain the upper limit of $\langle \sigma v \rangle$. The constraints on the DM annihilation cross-sections for $b\bar{b}$ and $\tau^+\tau^-$ are shown in Fig. 7 (no substructures). For comparison, the limits based on a combined analysis of dwarf spheroidal galaxies (dSphs) (Ackermann et al. 2015a) are also plotted in the figures. Our constraints on the DM $\langle \sigma v \rangle$ are much worse than the limits from the dSphs (see Fig. 7). In addition, we also perform a combined analysis of these 16 objects with and without the substructures. Even after considering the effect of substructures, the limits based on a stacking analysis cannot be compared to the constraints from dSphs.

5 CONCLUSION AND DISCUSSION

In this work, we have analysed 16 yr *Fermi*-LAT data to search for DM annihilation signal from the nearby galaxy clusters. We modelled the DM halo of each cluster by a NFW profile with and without the substructures. No statistically significant emission ($> 5\sigma$) is found in case of DM annihilations. However, the local significances of the signals in the directions of Coma and Perseus clusters are larger than 4σ. The best-fitting TS value is ~ 17.9 (20.6) for $\chi\chi \to b\bar{b}$ at $m_\chi \sim 30$ GeV for Coma without (with) the substructures. Furthermore, we found that the γ-ray emission in the centre of Coma cluster is significantly variable ($\sim 3.6\sigma$). In addition, the γ-ray excesses of the Coma region are located at different areas for the two periods. According to these facts, we can rule out the DM origin of the γ-ray excesses within the Coma region. The γ-ray emissions may originate from astrophysical processes or background fluctuations.

We report a tentative signal in the direction of Perseus cluster. The largest TS value is ~ 20.0 for $\chi\chi \to \tau^+\tau^-$ at $m_\chi \sim 38$ GeV. However, the corresponding annihilation cross-section is very large and has been excluded by the observations of dSphs. In addition, the peak TS value is not continuously growing with time. These indicate that the possible excess may not relate to DM annihilation. Moreover, a very strong γ-ray source is very near the centre of Perseus. Meanwhile, it is believed that there are a large number of relativistic particles in GCls (Brunetti & Jones 2014), which may generate γ-

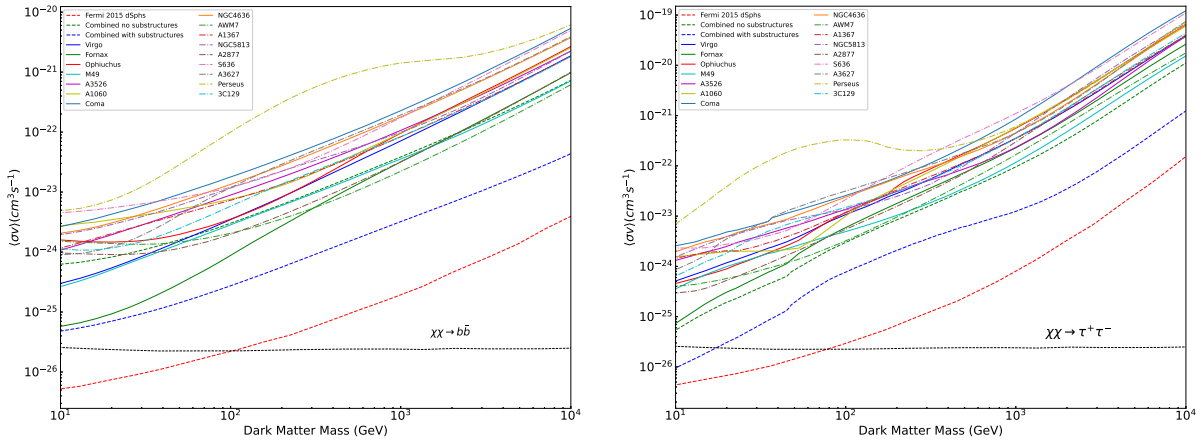

Figure 7. The 95 per cent C.L. upper limits of $\langle \sigma v \rangle$ for DM annihilation to $b\bar{b}$ (left) and $\tau^+\tau^-$ (right). The red dashed lines are the limits derived from a combined analysis of fifteen dwarf spheroidal galaxies (Ackermann et al. 2015a) and the black dashed line is the thermal relic cross-section (Steigman, Dasgupta & Beacom 2012).

rays by interacting with the intracluster medium. Hence, the excess may be from the central γ-ray point source, DM annihilations, astrophysical processes, or background fluctuations. Due to the signal not being statistically significant, we cannot determine the true origin at the moment. Nevertheless, detecting a possible γ-ray signal from Perseus cluster is very interesting. If coming from DM annihilation, the best-fitting DM mass ($\sim$ 38 GeV) for $\chi\chi \rightarrow \tau^+\tau^-$ is slightly lower than the energy of the γ-ray line signal ($\sim$ 43 GeV) (Fan et al. 2024). Although the connection between them is still unclear, it is also worth to pay more attention. The nature of the signal may be revealed by the *Fermi*-LAT and other γ-ray telescopes (Fan et al. 2022) in the future.

ACKNOWLEDGEMENTS

This work is supported in part by the National Key R&D Program of China (2021YFC22-3100, 2021YFC2203104), the National Natural Science Foundation of China (No. 12103001) and Anhui project (Z010118169).

DATA AVAILABILITY

The data underlying this article can be downloaded from the *Fermi*-LAT data server, https://fermi.gsfc.nasa.gov/cgi-bin/ssc/LAT/LATDataQuery.cgi.

REFERENCES

Abdollahi S. et al., 2022, ApJS, 260, 53
Ackermann M. et al., 2010, J. Cosmol. Astropart. Phys., 2010, 025
Ackermann M. et al., 2015a, Phys. Rev. Lett., 115, 231301
Ackermann M. et al., 2015b, ApJ, 812, 159
Atwood W. B. et al., 2009, ApJ, 697, 1071
Baghmanyan V., Zargaryan D., Aharonian F., Yang R., Casanova S., Mackey J., 2022, MNRAS, 516, 562
Bertone G., Hooper D., Silk J., 2005, Phys. Rep., 405, 279
Bonnivard V., Hütten M., Nezri E., Charbonnier A., Combet C., Maurin D., 2015, preprint (arXiv:1506.07628)
Brunetti G., Jones T. W., 2014, Int. J. Mod. Phys. D, 23, 1430007
Chang J. et al., 2017, Astropart. Phys., 95, 6
Charbonnier A., Combet C., Maurin D., 2012, Comput. Phys. Commun., 183, 656
Chen Y., Reiprich T. H., Bohringer H., Ikebe Y., Zhang Y. Y., 2007, A&A, 466, 805
Chen X.-B., Wang K., Huang Y.-Y., Zhang H.-M., Xi S.-Q., Liu R.-Y., Wang X.-Y., 2024, ApJL, 948, L47
Di Mauro M., Pérez-Romero J., Sánchez-Conde M. A., Fornengo N., 2023, Phys. Rev. D, 107, 083030
Diemand J., Kuhlen M., Madau P., 2007, ApJ, 657, 262
Diemand J., Kuhlen M., Madau P., Zemp M., Moore B., Potter D., Stadel J., 2008, Nature, 454, 735
Dugger L., Jeltema T. E., Profumo S., 2010, J. Cosmol. Astropart. Phys., 2010, 015
Fan Y. Z. et al., 2022, Acta Astron. Sin., 63, 27
Fan Y.-Z. et al., 2024, preprint (arXiv:2407.11737)
Feng J. L., 2010, Ann. Rev. Astron. Astrophys., 48, 495
Han J., Frenk C. S., Eke V. R., Gao L., White S. D. M., Boyarsky A., Malyshev D., Ruchayskiy O., 2012, MNRAS, 427, 1651
Hooper D., Profumo S., 2007, Phys. Rep., 453, 29
Huang X., Vertongen G., Weniger C., 2012, J. Cosmol. Astropart. Phys., 2012, 042
Hütten M., Combet C., Maurin D., 2019, Comput. Phys. Commun., 235, 336
Jeltema T. E., Profumo S., 2008, J. Cosmol. Astropart. Phys., 2008, 003
Jeltema T. E., Kehayias J., Profumo S., 2009, Phys. Rev. D, 80, 023005
Jungman G., Kamionkowski M., Griest K., 1996, Phys. Rep., 267, 195
Kataoka J. et al., 2010, ApJ, 715, 554
Liang Y.-F. et al., 2016, Phys. Rev. D, 93, 103525
Liang Y.-F., Xia Z.-Q., Xi S.-Q., Li S., Shen Z.-Q., Fan Y.-Z., 2018, preprint (arXiv:1801.01645)
Manna S., Desai S., 2024, J. Cosmol. Astropart. Phys., 2024, 023
Mattox J. R. et al., 1996, ApJ, 461, 396
Moliné Á., Sánchez-Conde M. A., Palomares-Ruiz S., Prada F., 2017, MNRAS, 466, 4974
Navarro J. F., Frenk C. S., White S. D. M., 1996, ApJ, 462, 563
Navarro J. F., Frenk C. S., White S. D. M., 1997, ApJ, 490, 493
Nolan P. L. et al., 2012, ApJS, 199, 31
Pinzke A., Pfrommer C., Bergström L., 2009, Phys. Rev. Lett., 103, 181302
Planck Collaboration XIII 2016, A&A, 594, A13
Sánchez-Conde M. A., Prada F., 2014, MNRAS, 442, 2271
Shen Z.-Q., Xia Z.-Q., Fan Y.-Z., 2021, ApJ, 920, 1
Springel V. et al., 2008, MNRAS, 391, 1685
Steigman G., Dasgupta B., Beacom J. F., 2012, Phys. Rev. D, 86, 023506
Thorpe-Morgan C., Malyshev D., Stegen C.-A., Santangelo A., Jochum J., 2021, MNRAS, 502, 4039
Xi S.-Q., Wang X.-Y., Liang Y.-F., Peng F.-K., Yang R.-Z., Liu R.-Y., 2018, Phys. Rev. D, 98, 063006

This paper has been typeset from a TEX/LATEX file prepared by the author.